ELSEVIER

PII: S0032-3861(96)00899-3

Polymer Vol. 38 No. 14, pp. 3505–3511, 1997

0032-3861/97/$17.00 + 0.00

The high-pressure crystallization behaviours and piezoelectricity of extended chain lamellar crystals of vinylidene fluoride trifluoroethylene copolymers with high molar content of vinylidene fluoride

T. Hattori, T. Watanabe*, S. Akama†, M. Hikosaka‡ and H. Ohigashi§
Department of Materials Science and Engineering, Faculty of Engineering, Yamagata University, Jonan 4-3-16, Yonezawa 992, Japan
(Received 9 February 1996; revised 19 June 1996)

In order to improve piezoelectric properties, high-pressure crystallization behaviours of copolymers of vinylidene fluoride (VDF) and trifluoroethylene with high molar content of VDF (86 and 94 mol%) were studied by high-pressure d.t.a., and high-pressure crystallized films were characterized by d.s.c., X-ray diffraction, and piezoelectric resonance. The pressure-phase diagrams showed that these polymers have the hexagonal (paraelectric) phase at high pressures. The films crystallized in this phase result in extended β-form crystals (β-ECCs) composed of planar zig-zag chains. Since their hexagonal phase appears in a lower temperature range as compared to the hexagonal phase of PVDF, well-developed β-ECC films were obtained easily without serious thermal degradation. The electromechanical coupling factor (k_t) of β-ECC film for thickness extensional mode is 0.19 for 86 mol% copolymer, and 0.15 for 94 mol% VDF copolymer. These copolymers retain stable piezoelectric activity up to the melting temperature (165 and 186°C for 86 and 94 mol% VDF copolymers, respectively). © 1997 Elsevier Science Ltd.

(Keywords: vinylidene fluoride trifluoroethylene copolymers; high-pressure crystallization; piezoelectricity)

INTRODUCTION

Strong thickness extensional piezoelectric effect and distinctive ferroelectric phenomena in vinylidene fluoride and trifluoroethylene copolymers, P(VDF/TrFE) with VDF content from 60 to 82 mol% are attributed to well-developed thick lamellar crystals of β-form(orthorhombic crystals with all-*trans* chains), which are regarded as extended chain crystals (β-ECCs)[1,2]. The β-ECCs are grown during annealing in the paraelectric phase, a disorder phase called a hexagonal phase or rotator phase[1–4]. The lamellar thickening through the sliding diffusion[5–7] in the hexagonal phase results in extended-chain crystals. The piezoelectric activity, quantitatively expressed by an electromechanical coupling factor k_t for the thickness extensional vibration mode, is proportional to the remanent polarization in a ferroelectric polymer film. Thus, one may expect that the copolymers composed of higher molar content of VDF will exhibit the higher piezoelectric activity: k_t of β-ECC P(VDF/TrFE) film with 80 mol% VDF is really 0.3[1,2], and k_t of PVDF is expected to be 0.37[8]. Moreover, the Curie temperature T_c increases with increasing VDF content[4,9], and, therefore, the temperature range in which the copolymers are usable as piezoelectric devices, will expand to higher temperature with increasing VDF content. However, since the paraelectric phase does not exist in the atmospheric pressure for the copolymers with VDF content higher than 90 mol%, they crystallize into the nonpiezoelectric, folded chain crystals of α-form composed of TGTḠ chains. For the copolymers of 82–90 mol% VDF, T_c is higher than the melting temperature T_m, but they still have a metastable hexagonal phase appearing in the cooling process from the melts or even in the heating process if they are nonpoled and include many conformational defects consisting of TG sequences. In this case they crystallize into ECCs comprising β-, γ- and α-forms, which can be transformed into pure β-form by repetitive polarization reversal[4].

In order to grow the β-ECCs in P(VDF-TrFE) with VDF content higher than 90 mol% and PVDF, and in order to grow β-ECCs more completely in the copolymers with 82–90 mol% VDF, we have to employ high-pressure crystallization techniques. This is because the partial derivative $(\partial T_c/\partial P)_T$ of the Curie temperature T_c against pressure P at constant temperature, is smaller than that of the melting temperature, $(\partial T_m/\partial P)_T$, and the paraelectric (hexagonal) phase, where ECCs are developed, appears above the triple point temperature T_{tri} and pressure

Present addresses: *Tohoku Epson Co., Ltd., Sakata 998-01, Japan; †Chemical Research Center, Central Glass Co., Ltd., Imafuku, Kawagoe 356, Japan; ‡Faculty of Integrated Arts and Sciences, Hiroshima University, Higashihiroshima 724, Japan
§To whom correspondence should be addressed

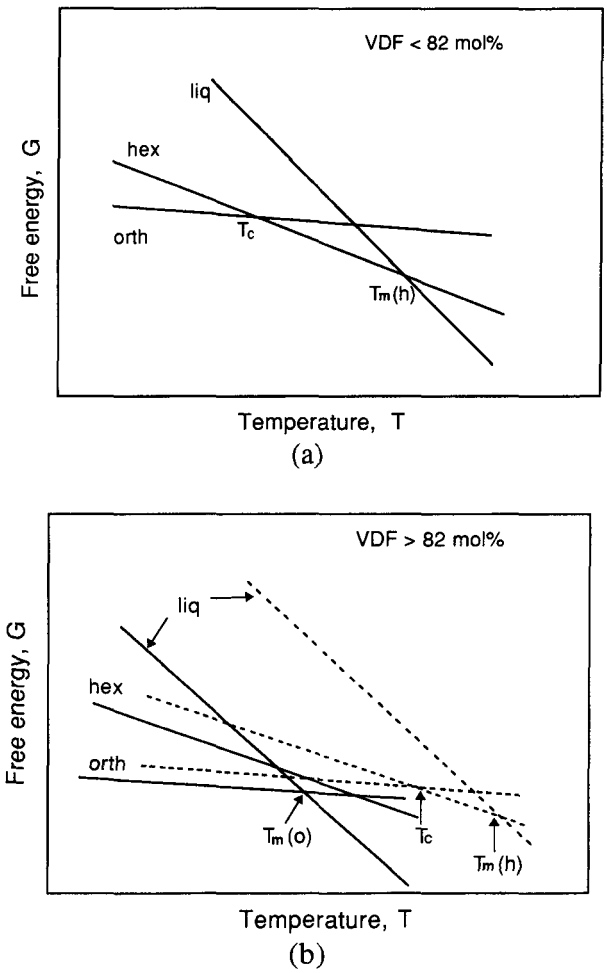

Figure 1 Temperature dependence of free energy G_i at atmospheric pressure for P(VDF/TrFE) with VDF less than 0.82 mol% (a) and larger than 82 mol% (b). Dotted lines in (b) show G_i at high pressure

P_{tri}. This situation is more directly shown by the Gibbs' free energies,

$$G_i = U_i + V_i P - S_i T \quad (1)$$

which are schematically depicted *Figure 1* for the orthorhombic ($i = o$), hexagonal ($i = h$) and liquid ($i = m$) phases of the copolymers with VDF molar contents less than 82% (*Figure 1a*) and larger than 82% (*Figure 1b*), where U_i, V_i and S_i are the internal energy, volume and entropy per unit mass of the ith phase, respectively[9,10]. In this figure we are taking into account that $S_m > S_h > S_o$ and $V_m > V_h > V_o$, and that U_o decreases with VDF content due to decrease in intermolecular distance, while U_h and U_m are not strongly dependent on VDF content. The temperature dependence of G_i under high pressure is also plotted in *Figure 1b*, indicating that the hexagonal phase emerges at high pressures.

In previous papers[11–13], we studied the phase diagram and crystallization behaviours of PVDF at high pressures, and piezoelectric properties of high-pressure crystallized PVDF films. A film composed of β-ECCs which were grown in the hexagonal phase at high pressures was found to retain its piezoelectric activity up to T_m (205°C), as expected. However, the magnitude of k_t realized (0.27) was considerably smaller than that expected for a single crystalline film ($k_t = 0.37$), mainly because the crystallization and polarization are not complete: the hexagonal phase appears at temperatures so high that the complete crystallization and poling are difficult due to intensive thermal degradation. Therefore, it is desirable to deal with the P(VDF/TrFE) copolymers with VDF content higher than 90 mol%, which have the hexagonal phase at lower pressures and temperatures than those necessary for the hexagonal phase in PVDF. The milder crystallization condition probably results in β-ECC films of higher quality. Doll and Lando[14] first studied high-pressure crystallization of P(VDF/TrFE) and showed that the copolymer of (91/9) crystallized in a planar zig-zag chain crystal (β-phase). At the time the existence of the hexagonal phase at high pressure was not conceived yet.

In a previous paper[9] we have reported that P(VDF/TrFE) with VDF content higher than 82 mol% really have the Curie point T_c higher than T_m, and that the piezoelectric activity of β-EECs crystallized at high pressure was persistent up to T_m. In the present paper we describe in detail the pressure–temperature (P–T) phase diagrams, structure and physical properties of high-pressure crystallized films of the P(VDF/TrFE) with VDF content of 86 and 94 mol%. Although the piezoelectric activity is not high as expected, the present study will give the basic information for further improvement of piezoelectric properties of PVDF homologues.

EXPERIMENTAL

P(VDF/TrFE) with VDF content of 86 and 94 mol%, kindly provided from Daikin Kogyo Co., Ltd, Osaka, Japan, were dissolved in dimethylformamide and cast into films 20–50 μm thick. The starting P(VDF/TrFE) films, clamped tightly between glass plates, were crystallized in a high-pressure vessel filled with silicone oil as a pressure transmission medium in two crystallization methods. In the first method (constant pressure method), original films were first heated up to 293°C under a constant pressure (320 MPa) and then cooled below 100°C at a rate of about 1°C min^{-1} before releasing the pressure. This method was employed for sample D (96/4). In the second method (constant temperature method or pressure quenching method), the original P(VDF/TrFE) films were melted at 150 MPa (initial pressure) and 255°C and then the pressure was increased up to 500 MPa at a fixed temperature. This method was employed for samples B (86/14) and E (96/4). Samples A (86/14) and C (94/6) were melt-crystallized at 0.1 MPa.

To obtain the P–T phase diagrams the phase transition temperature (T_c and T_m) were measured by differential thermal analysis (d.t.a.) at various pressures for the copolymers of β-ECCs once crystallized in a d.t.a. cell at high pressures. Differential scanning calorimetry (d.s.c.), scanning electron microscopy (SEM) and X-ray diffraction were employed to characterize the structure of high-pressure crystallized films.

The high-pressure crystallized films were poled by an a.c. field with a peak field of about 120–130 MV m^{-1} at 0.03 Hz and room temperature. The piezoelectric properties of the poled films were evaluated by analysing piezoelectric resonance curves measured with an impedance analyzer (YHP RF4191A), as described previously[2,15].

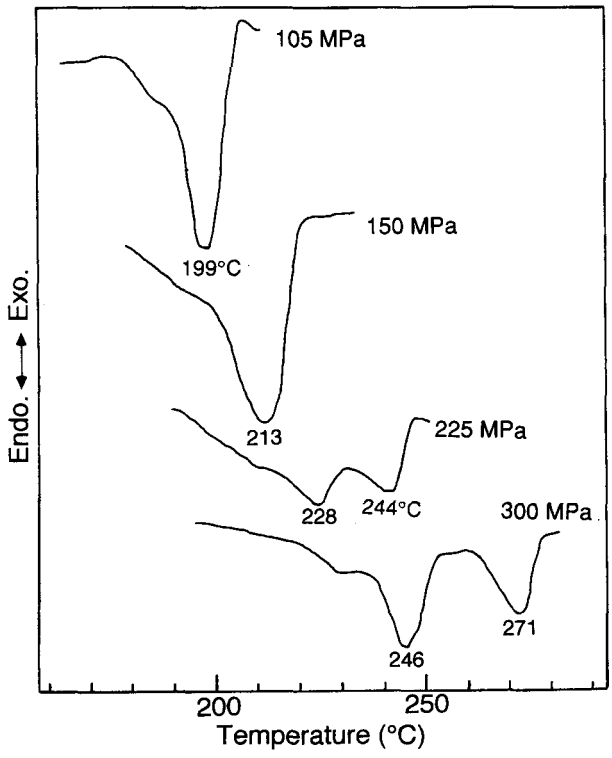

Figure 2 D.t.a. thermograms, recorded at 105, 150, 225 and 300 MPa in the heating process with heating rate at 5°C min^{-1}, of β-ECCs of P(VDF/TrFE) (86/14)

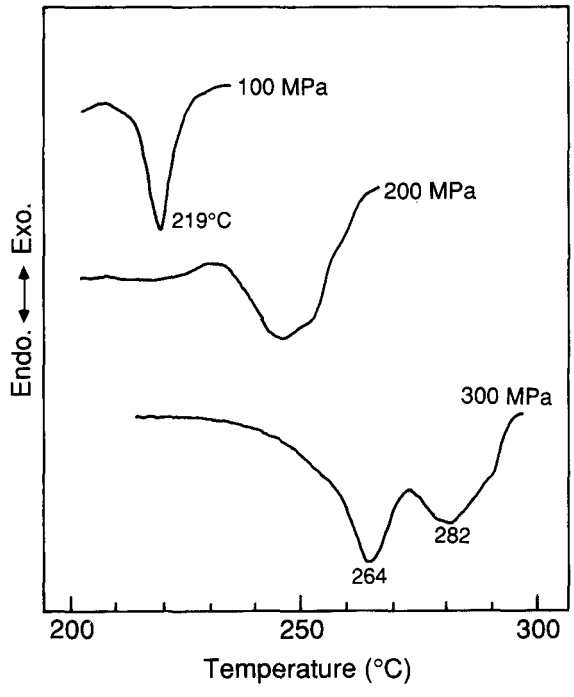

Figure 3 D.t.a. thermograms, recorded at 100, 200, and 300 MPa in the heating process with heating rate at 5°C min^{-1}, of β-ECCs of P(VDF/TrFE) (94/6)

RESULTS AND DISCUSSION

P–T phase diagrams

The high pressure d.t.a. thermograms, recorded at various pressures in the heating process with heating rate at 5°C min^{-1}, of P(VDF/TrFE) (86/14) and (94/6) are shown in *Figures 2* and *3*, respectively. The samples used in this experiment were crystallized at high pressure in advance to temperature scanning: in order to grow β-ECCs the original P(VDF/TrFE) films were once melted in the d.t.a. cell at 150 MPa and 255°C and then the pressure was increased slowly up to 500 MPa at 255°C. For P(VDF/TrFE) (86/14) a single endothermic peak corresponding to the melting point of β-ECCs (T_m) occurs at 199°C under 105 MPa (*Figure 2*) and shifts to the higher temperature side with increasing pressure. The single peak splits into double peaks at higher pressures, one corresponding to Curie temperature T_c (phase transition from ferroelectric or orthorhombic phase to paraelectric or hexagonal phase) and the other corresponding to the melting point $T_m(h)$ of the ECCs in the hexagonal phase. D.t.a. curves similar to those of

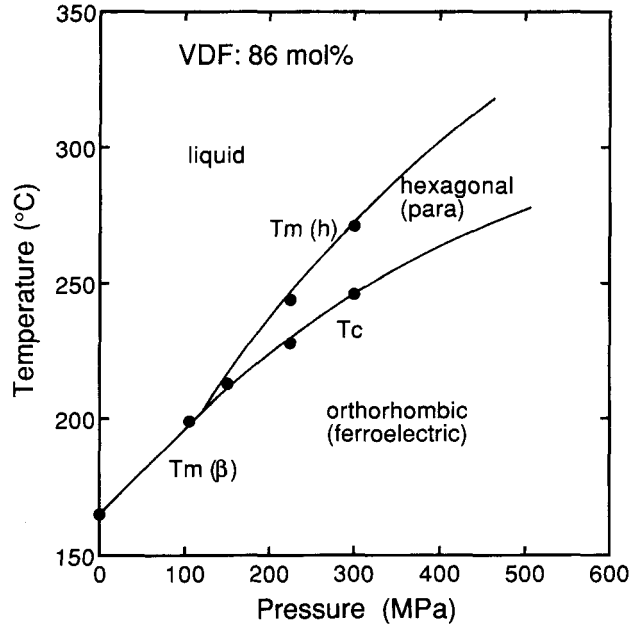

Figure 4 Pressure–temperature (P–T) phase diagram of P(VDF/TrFE) (86/14) (β-ECCs). The triple point is at 120 MPa and 205°C

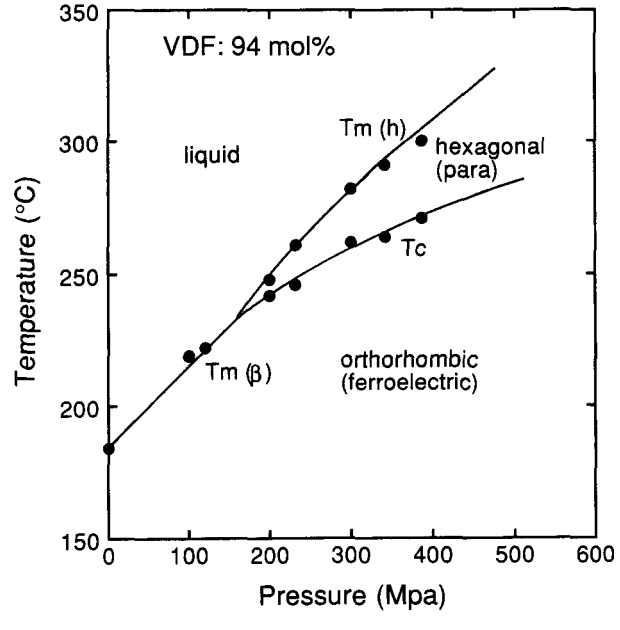

Figure 5 Pressure–temperature (P–T) phase diagram of P(VDF/TrFE) (94/6) (β-ECCs). The triple point is at 180 MPa and 230°C

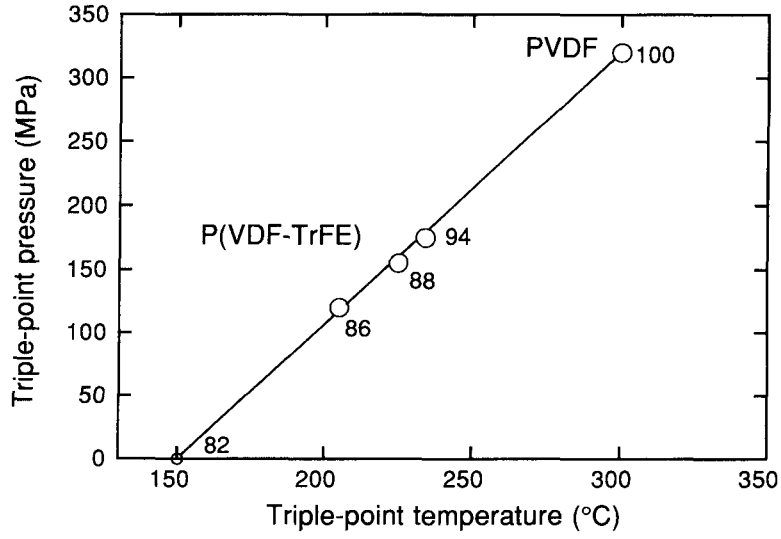

Figure 6 *P–T* plots of the triple points for β-ECCs of P(VDF/TrFE) and PVDF. Numerics represent the molar ratios (%) of VDF

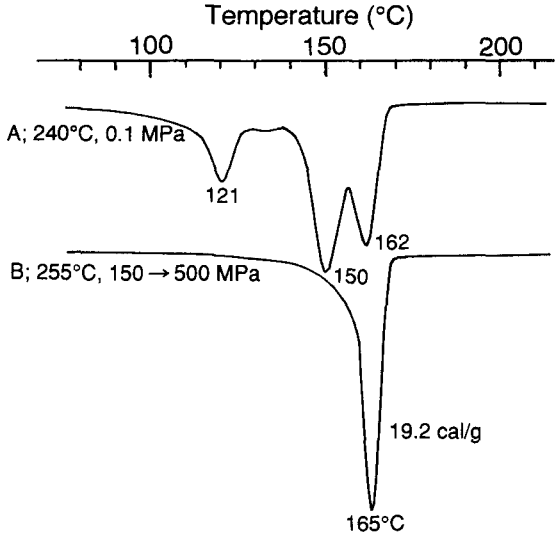

Figure 7 D.s.c. thermograms, recorded at 0.1 MPa, of P(VDF/TrFE) (86/14): samples A, melt crystallized at 0.1 MPa; sample B, crystallized at 255°C by constant temperature method with initial and final pressures 150 and 500 MPa, respectively

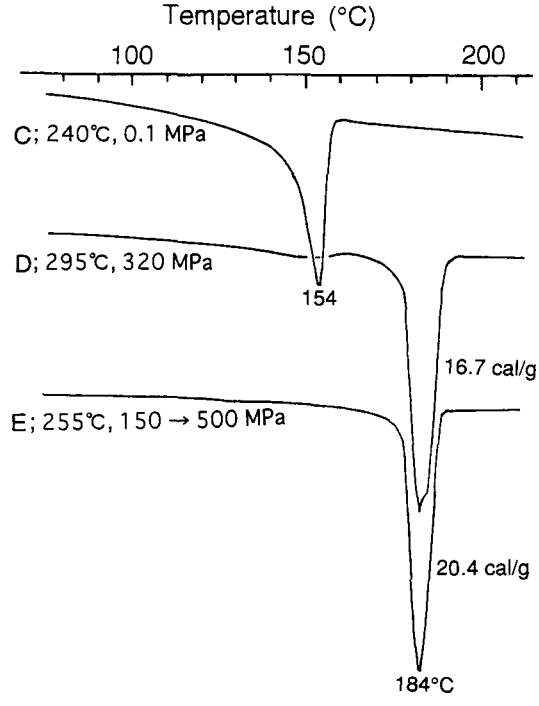

Figure 8 D.s.c. thermograms, recorded at 0.1 MPa, of P(VDF/TrFE) (94/6): samples C and D, crystallized by the constant pressure method at temperature and pressure as indicated; sample E, crystallized by the constant temperature method under the condition as indicated

P(VDF/TrFE) (86/14) are also observed at higher temperatures and pressures for P(VDF/TrFE) (94/6) (*Figure 3*). From these data we can obtain a pressure–temperature (*P–T*) phase diagram for the ECCs of P(VDF/TrFE) (86/14) and (94/6)[9] as shown in *Figures 4* and *5*, respectively. The triple point, at which the orthorhombic, hexagonal and liquid phases coexist, is at 120 MPa and 205°C for P(VDF/TrFE) (86/14), and is at 180 MPa and 230°C for P(VDF/TrFE) (94/6). *Figure 6* shows the plots of triple point on the *P–T* plane for P(VDF/TrFE)[4,9] and PVDF[12]. The triple point for P(VDF/TrFE) (82/18) is at 150°C and 0.1 MPa[2,4]. With increasing VDF content, it shifts linearly to the higher temperature and pressure side, reaching to 320°C and 300 MPa for PVDF.

D.s.c. thermograms

Figure 7 shows the typical d.s.c. thermograms recorded at 0.1 MPa for P(VDF/TrFE) (86/14) (samples A and B). In sample A the triple endothermic peaks at 121, 149 and 162°C correspond to the melting point of the ECCs of mixed phase of the α-, γ-, and β-forms as we discussed previously[4]. On the other hand, the single endothermic peak at 165°C in sample B corresponds to the melting point of ECCs composed of β-form only. This temperature is the same as T_m of β-ECCs converted from the mixed form ECCs by strong poling field[4].

Figure 8 shows d.s.c. thermograms of P(VDF/TrFE) (94/6) (samples C, D and E) recorded at 0.1 MPa. For comparison d.s.c thermograms of PVDF (samples F, G and H) are shown in *Figure 9*, where samples F, G and H were crystallized by the same procedures as for samples C, D and E, respectively. As previously reported, the endotherms of PVDF at 173–179°C are

attributable to the melting of α-form crystals, those at 203–206°C to the melting of ECCs having a mixed structure of β-form and γ-form, and those at 182–196°C to the melting of the folded chain lamellar crystals which have the mixed structure of β-form and γ-form[12]. The endotherm of P(VDF/TrFE) (94/6) at 154°C is attributable to the melting of α-form and possibly γ-form crystals and that at 184°C to the melting of β-ECCs, as described later. The difference in

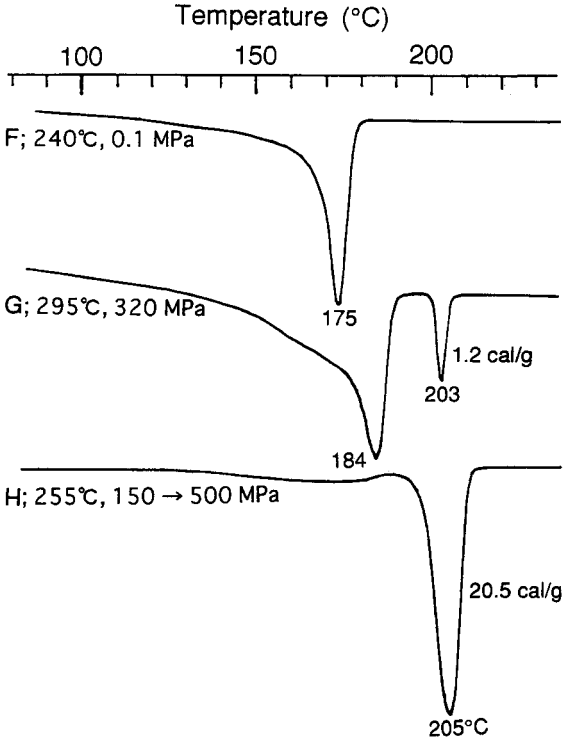

Figure 9 D.s.c. thermograms, recorded at 0.1 MPa, of high-pressure crystallized PVDF. Samples F, G and H were crystallized by the same procedures as for samples C, D and E in *Figure 8*, respectively

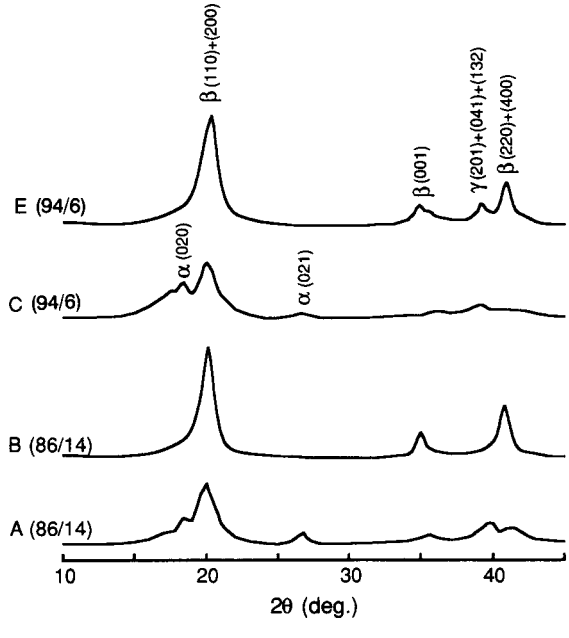

Figure 10 X-ray diffraction profiles of P(VDF/TrFE) (86/14) (samples A and B) and P(VDF/TrFE) (94/6) (samples C and E)

Figure 11 SEM image of fractured cross sections of high-pressure crystallized films of P(VDF/TrFE) (94/6) (sample E)

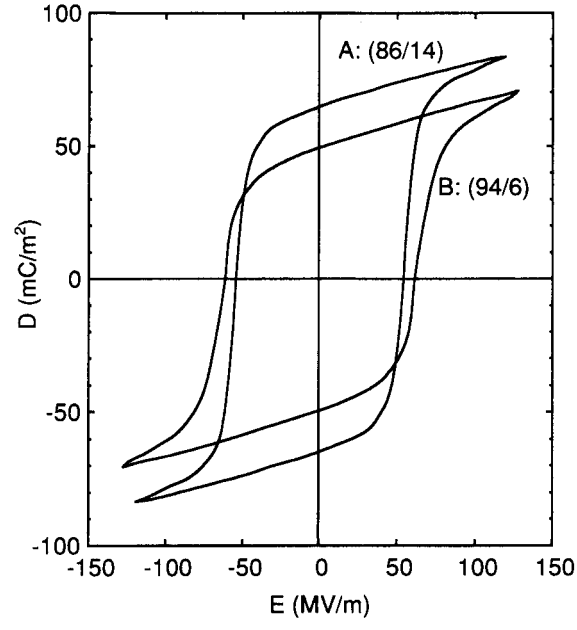

Figure 12 D–E hysteresis loops observed for high-pressure crystallized films of (A) P(VDF/TrFE)(86/14) (sample B), and (B) P(VDF/TrFE) (94/6) (sample D)

T_m of α-form crystals and β-ECCs is 30°C. This value is similar to the difference in PVDF.

The values of enthalpy change ΔH_m at T_m of β-ECCs in samples B (86/14), D (94/6), E (94/6), G (100/0) and H (100/0) are 19.2, 16.7, 20.4, 1.2 and 20.5 cal g^{-1}, respectively. ΔH_m is much larger in sample D than in sample G even though they were crystallized under the same condition. This fact indicated that the β-ECCs can be easily formed in P(VDF/TrFE) (94/6) at lower pressure and temperature as compared to those in PVDF.

X-ray diffraction profiles

Figure 10 shows X-ray diffraction profiles detected by the symmetrical reflection method for sample A (86/14), B (86/14), C (94/6) and E (94/6). Referring to the x-ray diffraction data of PVDF[16,17], the reflection peaks are characterized as follows; the reflection at 17.5° and 18.4° are assigned to the 100 and 020 reflections of α-form, respectively; 20.0–20.3° to 110α or 110β+

Table 1 Ferroelectric and piezoelectric properties of P(VDF/TrFE) and PVDF films

Material	T_m (°C)	T_c (°C)	k_t	v^i (km s^{-1})	P_r (mC m^{-2})	E_c (MV m^{-1})
P(VDF/TrFE)(75/25) (β-ECC)[a]	152	124	0.29	2.41	110	40
P(VDF/TrFE)(86/14) (β-ECC)[b]	165	(175)[h]	0.25	2.58	110	44
P(VDF/TrFE)(86/14) (β-ECC)[c]	165	(175)[h]	0.19	2.39	64	52
P(VDF/TrFE)(94/6) (β-drawn)[d]	154	–	0.19	2.27	–	–
P(VDF/TrFE)(94/6) (β-ECC)[e]	184	(210)[h]	0.15	2.49	50	62
PVDF (β-drawn)[f]	175	–	0.19	2.30	50	45
PVDF (β-ECC)[g]	205	(240)[h]	0.27	2.72	95	70

[a] Annealed in hexagonal phase at 0.1 MPa (ref. 2)
[b] Ref. 4
[c] Sample B poled by a.c. field at 25°C
[d] Ref. 4
[e] Sample D poled by a.c. field at 25°C
[f] Ref. 15
[g] Crystallized under high pressure and poled at high temperature (ref. 13)
[h] Thermodynamical T_c estimated by extrapolating T_c in the P–T phase diagram to 0.1 MPa (refs 9 and 12)
[i] Velocity of longitudinal sound propagating along the film normal (10–30 MHz)

200β or 110γ; 26.7° to 021α; 35.0° to 001β; 36.0–36.2° to 200α or 200γ; 39.0° to 132γ + 201γ + 041γ; and 40.9° to 220β + 400β.

The X-ray diffraction profiles in *Figure 10* indicate that P(VDF/TrFE) (86/14) crystallized from the melt at 0.1 MPa (sample A) is composed of a mixture of the α, β- and possibly γ-form crystals and that P(VDF/TrFE) (94/6) crystallized from the melt at 0.1 MPa (sample C) is composed of α- and γ-forms. Sample B(86/14) is composed of β-form crystals only, and E (94/6) is essentially of β-form plus a slight amount of γ-form. When these polymers are crystallized in the hexagonal phase, hexagonal ECCs grow extensively, which transform to β-ECCs on cooling below T_c. If the hexagonal phase appearing at high pressure is metastable, that is, when both the pressure and temperature is below or near the triple point and the hexagonal phase occurs from the melts, the resulting β-ECCs contain many $T_3GT_3\bar{G}$ conformation chain sequences (γ-form) to give the γ-form X-ray diffraction as in sample D. The mixed form ECCs are typically grown in PVDF crystallized at high pressure[12] or in P(VDF/TrFE) with VDF 82–90 mol% crystallized at 0.1 MPa[4]. The mixed form of ECCs can be converted to β-ECCs by poling treatment[4,12].

Morphology of β-ECCs

Morphology of β-ECCs was studied by SEM. *Figure 11* shows a SEM image of fractured cross section of sample E (94/6). Thick lamellar crystals about 0.1 μm thick, stacking parallel to each other, are observed all over the fractured cross section. These lamellar crystals were found to give an electron diffraction pattern typical for β-ECCs[3,4,12].

Polarization behaviour and piezoelectric properties

High-pressure crystallized films of β-ECCs of P(VDF/TrFE) with (86/14) and (94/6) exhibit typical ferroelectric nature and piezoelectricity. *Figure 12* shows room-temperature D–E hysteresis loops of samples B (86/14) and D (94/6). The remanent polarization P_r and coercive field E_c are 64 mC m^{-2} and 52 MV m^{-1}, respectively, for sample B (86/14) and 50 mC m^{-2} and 62 MV m^{-1}, respectively, for sample E (94/6). E_c increases with VDF content: E_cs of samples D and E are lower than E_c of high-pressure crystallized PVDF (70 MV m^{-1})[13], but larger than E_c of P(VDF/TrFE) (75/25) (40 MV m^{-1}). This may be related to the fact that the ratio of the orthorhombic unit cell dimension a/b increasingly deviates from the ratio of quasi-hexagonal lattice ($\sqrt{3}$) with increasing VDF content. The value of k_t evaluated from the strength of piezoelectric resonance is 0.19 for sample B (86/14) and 0.15 for sample D (94/6). *Table 1* lists the piezoelectric and related properties of the resulting films together with those of variously treated PVDF[13,15] and P(VDF/TrFE) films[2,4].

The k_t values of samples B and D are consistent with the values expected from P_r observed. [k_t is proportional to P_r with an empirical proportionality factor 3.0 (m^2 C^{-1})[8].] However, the observed P_r values are much smaller than those expected for an ideally oriented β-ECC film. The reason why is that, besides incomplete crystallization, the orientation of lamellar crystals in these films are random, which is in sharp contrast to the

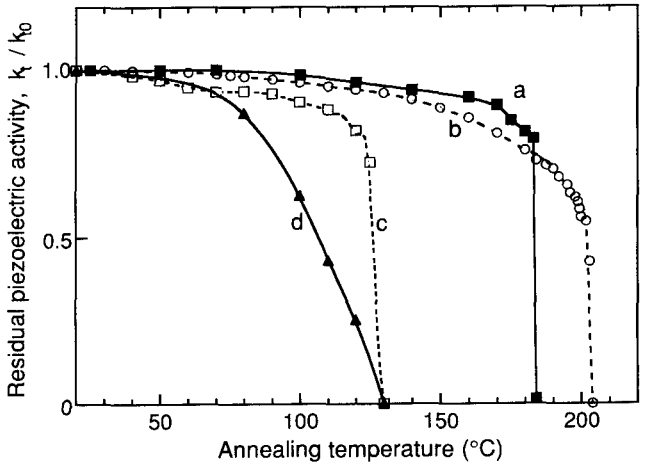

Figure 13 Thermal stability of piezoelectric activity in P(VDF/TrFE) and PVDF films, evaluated by the residual k_t value measured at 25°C after annealing for 10 min at respective temperature: (a) high-pressure crystallized P(VDF/TrFE) (94/6); (b) high-pressure crystallized PVDF[13]; (c) P(VDF/TrFE) (74/25)[8]; and (d) uniaxially stretched PVDF[4]

lamellar orientation in the films of P(VDF/TrFE) with VDF less than 82 mol%, where the lamellar planes of β-ECCs are apt to orient perpendicularly to the film planes, bringing about large polarization[1–3]. As in the case of high-pressure crystallized PVDF[13], the difficulty in the ferroelectric rotation of chains around the chain axis by application of external field at room temperature is probably an additional reason in the case of P(VDF/TrFE) (94/6). Therefore, more complete polarization in lamellar crystals might be achieved by poling at higher temperatures.

Thermal stability of piezoelectric activity

In order to evaluate the thermal stability of piezoelectric activity, the k_t value of high-pressure crystallized and poled film was measured at 25°C after annealing for 10 min at respective temperature. The residual k_t value measured at 25°C is shown in *Figure 13* as a function of annealing temperature for the high-pressure crystallized P(VDF/TrFE) (94/6) (sample D) (a) together with P(VDF/TrFE) (75/25)[8] (b), high-pressure crystallized PVDF[13] (c) and uniaxially stretched PVDF film[4] (d). It is clear that the piezoelectric activity in P(VDF/TrFE) (94/6) is stable up to the temperature near T_m. A sudden decrease in k_t near T_m or T_c occurs in common in P(VDF/TrFE) (75/25) (at T_c), and high pressure crystallized P(VDF/TrFE) (94/6) (at T_m) and PVDF (at T_m), all of which consist of well-developed β-ECCs. As reported previously[4,8], and as shown in *Figure 13*, β-phase films of PVDF and P(VDF/TrFE) (VDF content higher than 82 mol%), which are prepared by mechanical drawing, lose their piezoelectric activity in the temperature range much lower than the melting point. A mechanically drawn film is composed of small crystallites in which many defects are included. Such a film has a lot of evidence for unstable polarization: the coercive field E_c of drawn PVDF film is much lower than that of high-pressure crystallized PVDF (*Table 1*), and the remanent polarization P_r in drawn film is much smaller than the saturation polarization P_s. (The D–E hysteresis loop is not sharp.) Therefore, high-pressure crystallized P(VDF/TrFE) with high molar VDF content will be effective piezoelectric materials for devices working at high temperatures.

CONCLUSIONS

Thermodynamically stable hexagonal phase does not exist in P(VDF/TrFE) copolymers with VDF content higher than 82 mol% at atmospheric pressure. However, it appears at pressure and temperature higher than the triple point pressure (P_{tri}) and temperature (T_{tri}). In the hexagonal phase a P(VDF/TrFE) film with VDF content higher that 82 mol% is crystallized into a film composed of β-ECCs, whose piezoelectric activity is stable up to the temperature just below the melting point at atmospheric pressure. Since T_{tri} decreases with TrFE molar content, thermostable piezoelectric film of P(VDF/TrFE) can be prepared without thermal degradation under milder crystallization condition as compared with the condition for preparation of PVDF film composed of β-ECCs.

The piezoelectric activity of high-pressure crystallized films of P(VDF/TrFE) with VDF content of 86 and 94 mol% was found to be not so strong as expected. Improvement of piezoelectric properties may be achieved by seeking the crystallization condition for better growth of β-ECCs and the poling procedure for more complete polarization.

ACKNOWLEDGEMENTS

The authors are grateful to Dr E. Fukada for his encouragement throughout the work. They thank Daikin Kogyo Co., Ltd. for kindly supplying the polymers. This work was supported in part by the Grants-in-Aid for Scientific Research (No. 04555212 and No. 06452342) from the Ministry of Education, Science, Sports and Culture, Japan.

REFERENCES

1. Ohigashi, H. and Koga, K., *Jpn. J. Appl. Phys.*, 1982, **21**, L445.
2. Koga, K. and Ohigashi, H., *J. Appl. Phys.*, 1986, **59**, 2142.
3. Ohigashi, H., Akama, H. and Koga, K., *Jpn. J. Appl. Phys.*, 1988, **27**, 2144.
4. Koga, K., Nakano, N., Hattori, T. and Ohigashi, H., *J. Appl. Phys.*, 1990, **67**, 965.
5. Hikosaka, M., *Polymer*, 1987, **28**, 1257.
6. Hikosaka, M., *Polymer*, 1987, **30**, 459.
7. Hikosaka, M., Sakurai, K., Ohigashi, H. and Keller, A., *Jpn. J. Appl. Phys.*, 1994, **33**, 214.
8. Ohigashi, H., *Proc. 6th Int. Meeting on Ferroelectricity*, Kobe, 1985; *Jpn. J. Appl. Phys.*, 1985, **24**, (Suppl. 24-2), 23.
9. Ohigashi, H., Watanabe, T., Li, G. R, Hattori,T. and Takahashi, S., *Proc. 11th Symp. Ultrasonic Electronics*, Kyoto, 1990; *Jpn. J. Appl. Phys.*, 1991, **30**, (Suppl. 30-1), 111.
10. Ohigashi, H. and Hattori, T., *Ferroelectrics*, 1995 **171**, 11.
11. Ohigashi, H. and Hattori, T., *Jpn. J. Appl. Phys.*, 1989, **28**, L1612.
12. Hattori, T., Hikosaka, M. and Ohigashi, H., *Polymer*, 1996, **37**, 85.
13. Hattori, T., Kanaoka, M. and Ohigashi, H., *J. Appl. Phys.*, 1996, **79**, 2016.
14. Doll, W. W. and Lando, J. B., *J. Macromol.-Phys., B*, 1970, **4**, 897.
15. Ohigashi, H., *J. Appl. Phys.*, 1976, **47**, 949.
16. Hasegawa, R., Kobayashi, M. and Tadokoro, H., *Polymer J.*, 1972, **3**, 600.
17. Weinhold, S., Litt, M. H. and Lando, J. B., *Macromolecules*, 1980, **13**, 1178.